JOURNAL OF SOLID STATE CHEMISTRY **103,** 387–393 (1993)

Cation and Vacancy Distribution in Nonstoichiometric Hausmanite

JANUSZ KACZMAREK AND EMILIA WOLSKA*

Department of Magnetochemistry, Adam Mickiewicz University, Poznań, Grunwaldzka 6, PL-60-780 Poznań, Poland

Received June 17, 1992; in revised form August 28, 1992; accepted August 31, 1992

The defect structure of the synthetic anhydrous hausmanite Mn_3O_4 has been investigated by X-ray powder diffraction and chemical analysis. The integrated intensity ratios of X-ray reflections, the unit-cell constant values, and the Mn^{3+} content in samples evidence the nonstoichiometry of hausmanite. The degree of oxidation of manganese, Mn^{3+}/Mn^{2+}, varied in the ranges of 2.05 to 3.04. The main type of defects is the cation vacancies, the anionic sublattice remains virtually unaffected. The distribution of Mn^{3+} ions and of cation vacancies over the positions of both spinel cationic sublattices depends on the oxidation degree of manganese. For $Mn^{3+}/Mn^{2+} \leq 2.4$ the vacancies are created merely on the tetrahedral sites and for $Mn^{3+}/Mn^{2+} > 2.4$ the excess of vacancies is distributed at random over the tetrahedral and octahedral sites according to the formula $Mn^{2+}_{(8-3x)}Mn^{3+}_{2x}\square_x[Mn^{3+}_{16}]O_{32}$ for $x \leq 1/3$ and $Mn^{2+}_{(8-3x)}Mn^{3+}_{(3x/2-1/6)}\square_{(x/2+1/6)}[Mn^{3+}_{(97/6-x/2)}\square_{(x/2-1/6)}]O_{32}$ for $x > 1/3$. The lattice constants vary in the ranges $a = 0.8148$–0.8150 nm and $c = 0.9466$–0.9464 nm for Mn^{3+}/Mn^{2+} varying from 2.05 to 3.04. © 1993 Academic Press, Inc.

Introduction

Hausmanite, Mn_3O_4, is considered to be the most stable manganese oxide and can be obtained from any of the Mn oxides, hydrous oxides, or hydroxides, as well as from a variety of manganous salts (e.g., chloride, nitrate, sulfate) merely by thermal decomposition in air at about 1000°C. Mn_3O_4 can also be prepared by oxidation of an aqueous suspension of manganous hydroxide.

The low-temperature polymorph of hausmanite, α-Mn_3O_4, crystallizes in the tetragonal system, space group $I4_1/amd$. The unit cell with lattice constants $a = 0.576$ nm and $c = 0.944$ nm consists of four Mn_3O_4 units (*1*). It is, however, much more convenient to consider the crystal lattice of hausmanite as a tetragonally distorted spinel structure (space group $F4_1/ddm$). In that case the unit cell is twice the former one, with $a_s = \sqrt{2}a = 0.814$ nm and $c/a_s = 1.16$, containing 8 Mn_3O_4 units. The value of the oxygen parameter u has been determined to be equal to 0.375 (*2, 3*).

The unit-cell parameters reported for α-Mn_3O_4, measured at room temperature, differ slightly and vary within the ranges $a = 0.8136$–0.8150 nm (*4–8*) and $c = 0.942$–0.946 nm (*2, 5, 9, 10*). These divergences may be due to some extent to the different oxidation state of manganese and to the resulting lattice defects. The unit-cell parameters increase continually with increasing temperature, reaching the values of $a = 0.820$ nm and $c = 0.949$ nm at 1000°C (*5*). The reversible phase transformation of Mn_3O_4 from tetragonal (low-temperature,

*To whom correspondence should be addressed.

0022-4596/93 $5.00

Copyright © 1993 by Academic Press, Inc.
All rights of reproduction in any form reserved.

α-Mn_3O_4) to cubic (high-temperature, β-Mn_3O_4) symmetry takes place at 1150–1175°C.

The $t_{2g}^3e_g^1$ state for octahedral Mn(III) is subject to the Jahn–Teller effect, resulting in the distortion of $Mn^{III}O_6$ octahedra (with four Mn–O distances of 0.193 nm and two of 0.229 nm (*11*)) and changing the crystal structure from cubic to elongated tetragonal. Based on the above observations, the stoichiometric hausmanite, α-Mn_3O_4, at room temperature, may be regarded as a normal spinel (AB_2O_4); i.e., in the unit cell containing 32 oxide ions, 8 Mn^{2+} ions occupy the tetrahedral (*A*) and 16 Mn^{2+} ions the octahedral (*B*) sites (*8, 12, 13*).

Most references emphasize the tendency of hausmanite toward nonstoichiometry marked by the formation of oxygen-rich compounds compared to the Mn : O ratio in Mn_3O_4 (*14–17*). These departures from stoichiometry lead in consequence to defect structures, and Mn^{3+} for Mn^{2+} substitution may result in interstitial anions or in cation vacancy formation. The studies of Driessens (*12*) revealed the small effect of the oxygen pressure on the oxygen content in hausmanite, indicating a small number of anionic defects. The oxidation of manganese may then be equilibrated by the creation of cationic vacancies.

The first systematic studies on deviation from stoichiometry in hausmanite, $Mn_{3-\delta}O_4$, were undertaken by Dieckmann and Keller (*18–20*). The value of δ was determined thermogravimetrically, as a function of the oxygen activity, between 1000 and 1130°C for the low temperature phase (α-$Mn_{3-\delta}O_4$) and between 1200 and 1350°C for the high temperature phase (β-$Mn_{3-\delta}O_4$). A cation deficit was observed at high oxygen activities and a cation excess at low oxygen activities. It was concluded that in the temperature range investigated the dominant defect species in both phases are cation vacancies at high oxygen activities and interstitial manganese at low oxygen activities.

All of the studies cited above concerned cation and vacancy distributions in Mn_3O_4 at high temperatures only. No detailed investigations on defect structure and nonstoichiometry at room temperature have been reported. In this paper we present the results of X-ray powder diffraction measurements identifying the type of defects in the anhydrous hausmanite.

Experimental

Mn_3O_4 samples were prepared by thermal decomposition of $MnCO_3$, $MnSO_4$, and MnO_2 (analytical grade reagents) and of "low temperature $Mn_3O_4 \cdot aq$" (obtained by oxidation of $Mn(OH)_2$) at 900–1100°C during 3 hr in air. The variety of reactants used, as well as the decomposition temperatures, led to the formation of hausmanite samples with different oxidation degree of manganese (see Table I). The X-ray powder diffraction patterns indicated that the samples were monophasic (Fig. 1).

For the quantitative chemical analysis the samples were dissolved in hydrochloric acid. The content of Mn^{2+}-, Mn^{3+}-ions and of total manganese was determined by both iodimetric titration and EDTA back-titration with Zn^{2+} solution using Eriochrome Black T as indicator. The limit of error for the determination of Mn^{2+} and Mn^{3+} was $\pm 0.2\%$.

X-ray powder diffraction studies were performed with a TUR-M61 diffractometer equipped with a HZG-3 horizontal goniometer and proportional counter employing the Mn-filtered FeKα radiation. For the precise determination of lattice parameters the X-ray reflections in the range Θ = 28°–43° were recorded by step scanning, using Θ increments of 0.01° and a fixed counting time of 60 sec/step. The limit errors for *a* and *c* unit-cell constant detcr-

TABLE I

PREPARATION DETAILS AND ANALYTICAL DATA OF SYNTHETIC ANHYDROUS HAUSMANITE SAMPLES

Sample number	Precursor Mn-compound	Decomposition temperature (°C)	Chemical composition (wt.%)			Oxidation degree		Cation vacancies, $\square_{Mn}$/unit-cell
			Mn^{3+}	Mn^{2+}	O^{2-}	Mn^{3+}/Mn^{2+}	x in Mn^{x+}	
1	$MnCO_3$	1000	48.42	23.57	28.01	2.05	2.672	0.05
2	$MnSO_4$	1100	49.34	22.54	28.12	2.19	2.687	0.18
3	$MnSO_4$	1100	49.68	22.16	28.16	2.24	2.692	0.23
4	MnO_2	1100	49.75	22.09	28.16	2.25	2.692	0.23
5	$Mn_3O_4 \cdot aq$	1000	50.24	21.54	28.22	2.33	2.700	0.30
6	$MnCO_3$	1100	50.65	21.08	28.27	2.40	2.707	0.35
7	$MnCO_3$	900	51.83	19.77	28.40	2.62	2.724	0.50
8	$MnCO_3$	1100	53.71	17.68	28.61	3.04	2.752	0.75

mination were $\Delta a = \pm 0.0001$ nm and $\Delta c = \pm 0.0003$ nm.

The measurements of the integrated intensities of the X-ray lines were made by the continuous-averaging scan technique at a scan rate of 0.25°/min. To avoid the effect of preferred orientation of crystallites a brass sample holder with a thin film window was used. The changes in the reflection intensities ratios $I(111)/I(511)$, $I(202)/I(511)$, and $I(404)/I(400)$ were measured and compared with the intensity ratios calculated for models of the Mn_3O_4 structure with different cation and vacancy distributions.

For the hausmanite regarded as tetragonally distorted normal spinel, AB_2O_4, assuming the oxygen parameter $u = 0.375$ (*2*, *3*), the relation between the structure factors (F_{hkl}) and the form factors (f_A, f_B, and f_O)

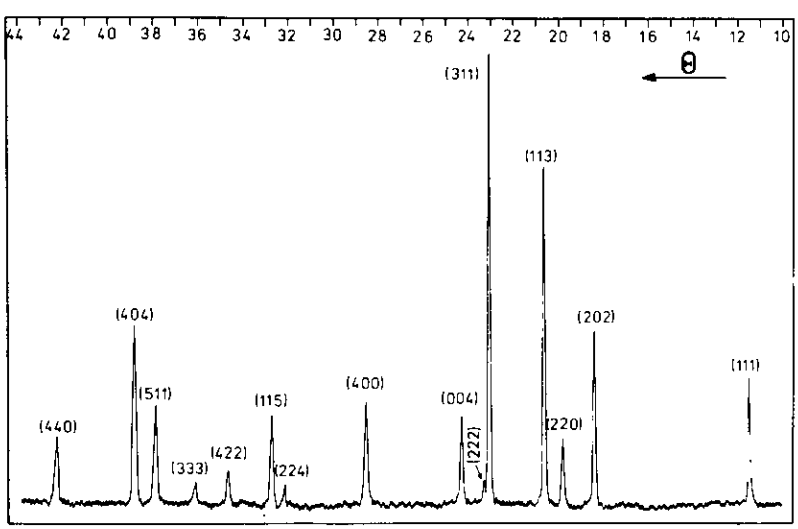

FIG. 1. X-ray powder diffraction pattern of anhydrous hausmanite—sample 6. *hkl* indices correspond to the tetragonal spinel unit cell; Fe$K\alpha$ radiation.

calculated for the Θ range of 10°–43° are given by the expressions

(hkl)	$\lvert F_{hkl}\rvert^2$
(111)	$32(2f_B - f_A)^2$
(202),(220),(224),(422)	$64f_A^2$
(113),(115),(311),(333),(511)	$32(f_A + 2f_B)^2$
(222)	$256(2f_O - f_B)^2$
(004),(400)	$64(2f_B - f_A + 4f_O)^2$
(404),(440)	$64(2f_B + f_A + 4f_O)^2$

(1)

Theoretical intensities were calculated as $I_{hkl} = |F_{hkl}|^2 \times p \times$ (L.P.). The values of atomic scattering factors, multiplicity factors (p), and Lorenz polarization factors (L.P.) were taken from the International Tables for X-ray Crystallography (*21*). The limit errors of the intensity measurements were $\Delta I_{111/511} = \pm 2\%$, $\Delta I_{202/511} = \pm 3\%$, and $\Delta I_{404/400} = \pm 5\%$.

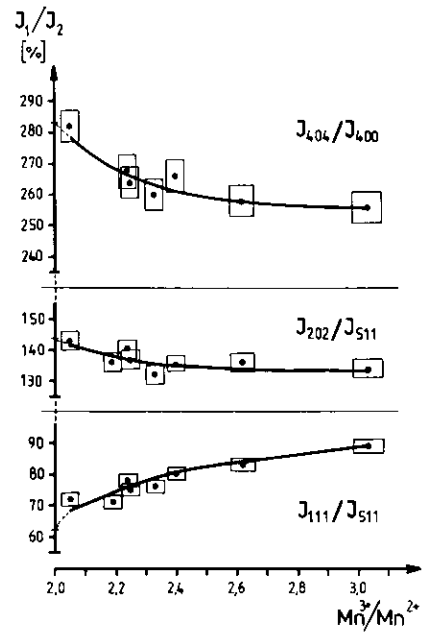

FIG. 2. Experimental values of the integrated intensity ratios of X-ray lines plotted against the oxidation degree of manganese, Mn^{3+}/Mn^{2+}.

Results and Discussion

As was already mentioned all preparations of hausmanite obtained during thermal treatment were monophasic and very well crystallized. Figure 1 shows the X-ray powder pattern of an average sample (number 6). Electron microscopic observations revealed the cubooctahedric crystallites.

The content of O^{2-} ions per unit cell was calculated on the bases of pycnometric density measurements, chemical analysis, and unit cell volume determined from X-ray diffraction (e.g., for sample 6, $\rho_{20°} = 4.74$ g·cm^{-3}, $V = 629.0 \cdot 10^{-24}$ cm^3). The values of ΣO^{2-}/unit cell obtained were 31.7 and 31.8.

The degree of oxidation of manganese, Mn^{3+}/Mn^{2+}, in the Mn_3O_4 samples was variable but as a rule higher than the stoichiometric one and comprised the values of $2.05 \leq Mn^{3+}/Mn^{2+} \leq 3.04$.

The occurence of supplementary Mn^{3+} ions in the presence of the unaffected anionic sublattice was the main reason of the cation vacancy formation according to the relation.

$$3Mn^{2+} = 2Mn^{3+} + \square_{Mn}. \qquad (2)$$

The numbers of cationic vacancies per unit cell derived from chemical analysis of samples are presented in Table I. Calculations have been made on the assumption that ΣO^{2-}/unit cell = 32.

Variation of the X-ray line intensity appears to be proportional to the degree of oxidation of manganese, which was the main factor in the vacancy creation, and therefore the measured values of the intensity ratios were plotted against the Mn^{3+}/Mn^{2+} ratio. Figure 2 shows these results with the marked limits of error. The $I(111)/I(511)$ values increase whereas $I(202)/I(511)$ and $I(404)/I(400)$ decrease with the increase of the oxidation degree of manganese in preparations. Assuming that the form fac-

tors $f_{Mn^{3+}} \approx f_{Mn^{2+}}$, the changes observed may be attributed to the formation of cation vacancies. Consideration of the structure factor values in Eq. (1) indicates that the cation vacancies are formed mainly in tetrahedral positions.

In order to determine the most probable vacancy distribution calculations of the X-ray line intensity ratios were performed for the following defect structure models of hausmanite:

I. The cation vacancies are located in the *A* sublattice only. The Mn^{2+} ions and the excess of Mn^{3+} ions occupy the tetrahedral sites; the *B* sublattice and the anionic sublattice are undefected. For this model two possibilities of cation and vacancy distribution were assumed: Ia. Vacancies for the oxidation degree $Mn^{3+}/Mn^{2+} \leq 2.4$ are distributed over the *A* sites and for $Mn^{3+}/Mn^{2+} > 2.4$ over the *B* sites; Ib. Vacancies for $Mn^{3+}/Mn^{2+} > 2.4$ are randomly distributed on both *A* and *B* sublattices.

II. The cation vacancies occupy the *B* sites only. The *A* sublattice and the anionic one are undefected with the Mn^{2+} and Mn^{3+} ions on *A* sites.

III. Vacancies are randomly distributed and devided between both *A* and *B* cation sublattices, i.e., $1/2\ \square_{Mn}$ and Mn^{3+} ions on *B* sites (16 positions) and $1/2\ \square_{Mn}$, Mn^{2+} and remaining Mn^{3+} on the *A* sites (8 positions).

IV and V models correspond to I and III respectively, with assumed ΣO^{2-}/unit cell = 31.5.

For stoichiometric hausmanite ($Mn^{3+}/Mn^{2+} = 2.0$) theoretical intensity ratios are $I(111)/I(511) = 62.39\%$; $I(202)/I(511) = 143.78\%$; and $I(404)/I(400) = 283.29\%$.

Figure 3 presents the intensity ratios calculated for the models I–V plotted as a function of the oxidation degree, Mn^{3+}/Mn^{2+}, compared to the intensity ratios measured taken from Fig. 2. Experimental results confirm that the mechanism I–Ib is operative. For the oxidation degree of manganese in the ranges $2.0 \lesssim Mn^{3+}/Mn^{2+} \lesssim 2.4$ the cation vacancies are created in the *A* sublattice in consequence of the oxidation of Mn^{2+} to Mn^{3+} on tetrahedral sites. The "saturation" of the *A* sublattice with the cation vacancies appears for $1/3\ \square_{Mn}$/unit-cell approximately and for $Mn^{3+}/Mn^{2+} > 2.4$ further cation vacancies are randomly distributed over the tetrahedral and octahedral positions. The $I(111)/I(511)$ and $I(202)/I(511)$ intensity ratios measured fit the I–Ib model particularly well. The residual factor $R = 0.0039$. These

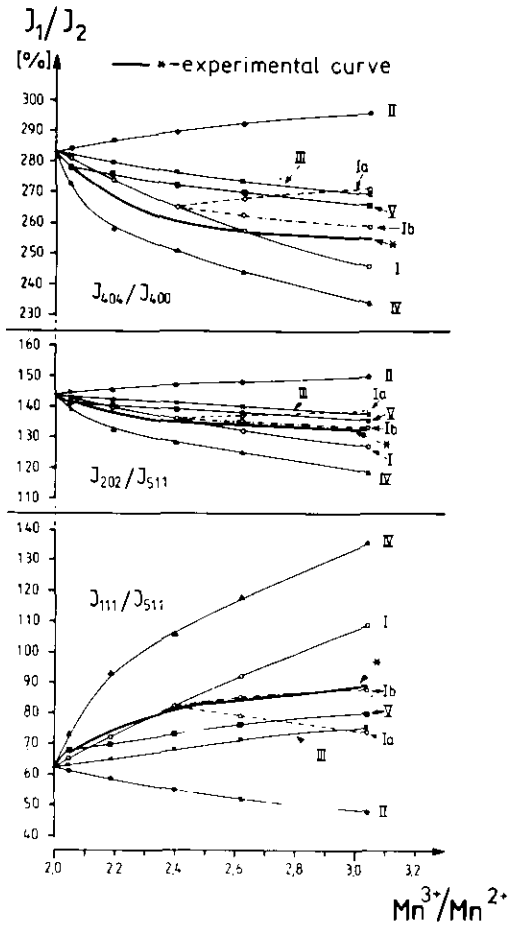

FIG. 3. X-ray line intensity ratios as a function of the oxidation degree of manganese, Mn^{3+}/Mn^{2+}, calculated for different cation and vacancy distributions (curves I–V). See text.

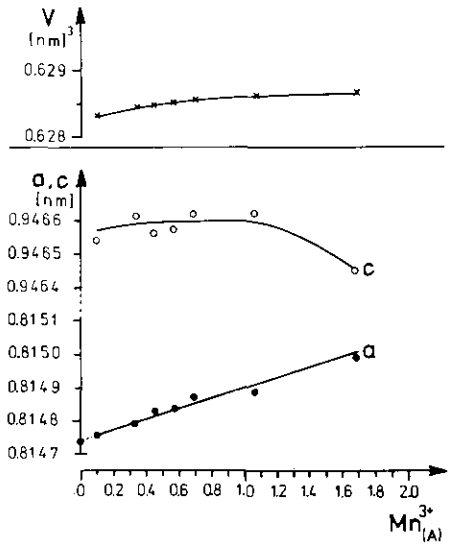

FIG. 4. Lattice constants and volume of the tetragonal spinel unit cell of hausmanite plotted as a function of Mn^{3+} content in tetrahedral sites.

data show clearly as well that the assumption of undefected or very slightly defected ($\square_A \leqslant 0.5$/unit cell) anionic sublattice was correct.

For nonstoichiometric anhydrous hausmanite, considered as a normal spinel $A_8[B_{16}]O_{32}$, the following general formula can be suggested:

$$Mn^{2+}_{(8-3x)}Mn^{3+}_{2x}\square_x[Mn^{3+}_{16}]O_{32} \qquad (3)$$

for $2.0 \leq Mn^{3+}/Mn^{2+} \leq 2.4$ and $x \leq 1/3$, and

$$Mn^{2+}_{(8-3x)}Mn^{3+}_{(5x/2-1/6)}\square_{(x/2+1/6)}[Mn^{3+}_{(97/6-x/2)}\square_{(x/2-1/6)}]O_{32} \qquad (4)$$

for $Mn^{3+}/Mn^{2+} > 2.4$ and $x > 1/3$, where x is the number of cation vacancies per unit cell. Substituting $Mn^{3+}/Mn^{2+} = \alpha$, the relation between the number of cation vacancies (x) and the oxidation degree of manganese (α) may be written as

$$x = \frac{8(\alpha - 2)}{3\alpha + 2}. \qquad (5)$$

The values of lattice constants and the unit cell volume of a tetragonal spinel unit cell of the hausmanite samples determined by x-ray powder diffraction are presented in Fig. 4, plotted as a function of the Mn^{3+} content in tetrahedral spinel positions. Table II contains these unit cell parameters together with the number of vacancies per unit cell and their distribution over the A and B cation sublattices. Although the a and c parameters change only slightly with the increase of the oxidation degree of manganese, some distinct regularities can be observed. The a parameter increases with the

TABLE II

CATION AND VACANCY DISTRIBUTION OVER THE TETRAHEDRAL (A) AND OCTAHEDRAL (B) SPINEL SITES, LATTICE PARAMETERS, AND UNIT-CELL VOLUME OF SYNTHETIC ANHYDROUS HAUSMANITE SAMPLES

Oxidation degree, Mn^{3+}/Mn^{2+}	Cation vacancies		Mn^{3+} ions		Lattice constants (nm)		Unit-cell volume (nm^3)
	A	B	A	B	a (±0.0001 nm)	c (±0.0003 nm)	
2.05	0.054	0	0.107	16	0.81476	0.94654	0.6283
2.19	0.178	0	0.352	16	0.81479	0.94661	0.6284
2.25	0.225	0	0.464	16	0.81483	0.94656	0.6285
2.33	0.296	0	0.591	16	0.81484	0.94657	0.6285
2.40	0.354	0	0.697	16	0.81487	0.94662	0.6286
2.62	0.430	0.075	1.083	15.925	0.81489	0.94662	0.6286
3.04	0.550	0.196	1.691	15.804	0.81499	0.94645	0.6286

increase of Mn^{3+} content in tetrahedral sites despite of the increase of cation vacancies in the *A* positions. It may be explained by the Jahn–Teller distortion which appears as a flattening of the oxygen tetrahedra containing Mn^{3+} ions. The occurrence of cation vacancies in the octahedral sites, i.e., the decrease in Mn^{3+} content on *B* sites, attenuates the Jahn–Teller effect on the oxygen octahedra responsible for the tetrahedral distortion of spinel lattice and the *c* parameter decreases, but only for high Mn^{3+} content in the Mn_3O_4 lattice. The result of precise measurement of the unit cell parameters confirms indirectly the correctness of the assumed model of structure of nonstoichiometric anhydrous hausmanite.

References

1. H. STRUNZ, "Mineralogische Tabellen," Akademische Verlagsgesellschaft, Leipzig (1977).
2. G. AMINOFF, *Z. Kristallogr.* **64,** 475 (1926).
3. E. J. W. VERWEY AND J. H. DE BOER, *Rec. Trav. Chim. Pays-Bas* **55,** 531 (1936).
4. A. P. B. SINHA, N. R. SANJANA, AND A. B. BISWAS, *Acta Crystallogr.* **10,** 439 (1957).
5. H. J. VAN HOOK AND M. L. KEITH, *Am. Mineral.* **43,** 69 (1958).
6. K. S. IRANI, A. P. SINHA, AND A. BISWAS, *J. Phys. Chem. Solids* **23,** 711 (1962).
7. B. BOUCHER, R. BUHL, AND M. PERRIN, *J. Phys. Chem. Solids* **32,** 2429 (1971).
8. B. CHARDON AND F. VIGNERON, *J. Magn. Magn. Mater.* **58,** 128 (1986).
9. J. B. GOODENOUGH AND A. L. LOEB, *Phys. Rev.* **98,** 391 (1955).
10. K. J. SATOMI, *J. Phys. Soc. Jpn.* **16,** 258 (1961).
11. R. NORRESTAM, *Acta Chem. Scand.* **21,** 2871 (1967).
12. F. C. DRIESSENS, *Inorg. Chim. Acta* **1,** 193 (1967).
13. R. G. BURNS, "Mineralogical Application to Crystal Field Theory," Cambridge Univ. Press, Cambridge (1970).
14. W. FEITKNECHT AND W. MARTI, *Helv. Chim. Acta* **28,** 129 (1945).
15. W. FEITKNECHT, P. BRUNNER, AND H. R. OSWALD, *Z. Anorg. Allg. Chem.* **316,** 154 (1962).
16. J. D. HEM, *Geochim. Cosmochim. Acta* **45,** 1369 (1981).
17. J. W. MURRAY, J. G. DILLARD, R. GIOVANOLI, H. MOERS, AND W. STUMM, *Geochim. Cosmochim. Acta* **49,** 463 (1985).
18. R. DIECKMANN AND M. KELLER, *Mater. Sci. Monogr. A* **28,** 109 (1985).
19. R. DIECKMANN AND M. KELLER, *NATO ASI Series B* **129,** 297 (1985).
20. M. KELLER AND R. DIECKMANN, *Ber. Bunsenges. Phys. Chem.* **89,** 1095 (1985).
21. "International Tables for X-ray Crystallography" (N. F. M. Henry and K. Lonsdale, Eds.), Vol. III, Kynoch, Birmingham (1962).